

High-severity and short-interval wildfires limit forest recovery in the Central Cascade Range

SEBASTIAN U. BUSBY¹  † KEVAN B. MOFFETT,² AND ANDRÉS HOLZ  ¹

¹*Department of Geography, Portland State University, 1721 SW Broadway, Portland, Oregon 97201 USA*

²*School of the Environment, Washington State University, Vancouver, Washington 98686 USA*

Citation: Busby, S. U., K. B. Moffett, and A. Holz. 2020. High-severity and short-interval wildfires limit forest recovery in the Central Cascade Range. *Ecosphere* 11(9):e03247. 10.1002/ecs2.3247

Abstract. Increasing forest fuel aridity with climate change may be expanding mid-to-high-elevation forests' vulnerability to large, severe, and frequent wildfire. Long-lasting changes in forests' structure and composition may occur if dominant tree species are poorly adapted to shifting wildfire patterns. We hypothesized that altered fire activity may lower existing forest resilience and disrupt the recovery of upper-montane and subalpine conifer forest types. We empirically tested this hypothesis by quantifying post-fire forest structure and conifer tree regeneration after spatially large, severe, and rapidly repeated wildfires (<12-yr interval) in the Central Cascade Range in the U.S. Pacific Northwest. Post-fire conifer regeneration was generally very poor among plots that experienced either a single high-severity fire or rapid reburn, driven primarily by lack of proximate seed source. Pre-fire dominant, shade-tolerant species' abundance was highly negatively correlated with increasing seed source distances and dry, exposed post-fire environmental conditions. In rapidly reburned plots, the order of burn severity was critical and promoted establishment of all conifer species, if low-then-high severity, or primarily fire-adapted pines, if high-then-low severity. Our findings suggest that these forests, affected by expansive high-severity and/or short-interval wildfire, may transition into a patchy, low-density, pine-dominated forest state under future warming trends. These emerging, early seral ecosystems will incorporate more fire-adapted tree species, lower tree densities, and more non-forest patches than prior forests, likely expanding their resilience to anticipated increases in fire frequency. If future larger, more severe, and more frequent wildfire patterns manifest as expected in the Cascade Range, previously denser, moist mid-to-high-elevation forests may begin resembling their drier, lower-elevation mixed-conifer counterparts in structure and composition.

Key words: Cascade Range; conifers; high-severity wildfire; Mt. Adams; Mt. Jefferson; post-fire forest recovery; post-fire forest structure; reburn; short-interval wildfire; subalpine; upper-montane.

Received 2 January 2020; **revised** 23 May 2020; **accepted** 9 June 2020; **final version received** 23 July 2020. Corresponding Editor: Carrie R. Levine.

Copyright: © 2020 The Authors. This is an open access article under the terms of the Creative Commons Attribution License, which permits use, distribution and reproduction in any medium, provided the original work is properly cited.

† **E-mail:** sebusby@pdx.edu

INTRODUCTION

Wildfire is the most pervasive natural disturbance agent shaping temperate forest ecosystems. Within climatically cool and wet, mid-to-high-elevation conifer forests, shifts in mountain snowpack dynamics and seasonal temperature are increasing summertime fuel aridity and may alter subsequent wildfire behavior (Abatzoglou

and Williams 2016, Westerling 2016, Gergel et al. 2017). Altered fire regimes may limit the recovery of existing forest compositions following fire events, synergize with other disturbances, and be a catalyst for rapid ecosystem change when ecological legacies desynchronize with disturbance patterns (Johnstone et al. 2016). In the Cascade Range in the U.S. Pacific Northwest (PNW) region, concerns exist around the resilience of

mid-to-high-elevation forests, to absorb stress and recover following recently observed and predicted increases in fire frequency, severity, and size (Cansler and McKenzie 2014, Dennison et al. 2014, Abatzoglou et al. 2017, McKenzie and Litell 2017, Reilly et al. 2017). These forests have historically experienced relatively infrequent fire (Agee 1993, Tepley et al. 2013) and so are dominated by shade-tolerant, obligate seeding conifer species (*Abies*, *Tsuga*, *Picea*, genera) that require long fire-free intervals and/or proximate live seed sources to re-establish (Franklin and Hemstrom 1981, Agee 1993). Thus, dominant forest compositions in the upper-montane and subalpine zones of the Cascades may be poorly adapted to fire regimes that may be shifting to larger, more severe, and more frequent fires (Enright et al. 2015, Halofsky et al. 2020). Historically infrequent wildfire in these cool and moist forest types has limited the number of natural experiments available to study; thus, little research has yet to empirically evaluate these concerns.

Forest recovery following shifts in wildfire behavior has been widely documented, however, across the climatically drier and warmer forests in the western United States (Naficy et al. 2010, Collins et al. 2011, Merschel et al. 2014). In many dry forest types, increased fire severity and extent over the historical range of variability has occurred due to increased forest densities and fuel loads from 20th-century fire exclusion legacies (Hessburg et al. 2019). This has raised concerns over long-term forest resilience across many arid to semi-arid environments adapted to frequent and low-to-mixed-severity fires. In dry forests, recent trends of expansive high-severity fire (i.e., most or all canopy trees are killed) continue to limit conifer seed availability and thus post-fire tree regeneration. Low seed availability has been further compounded by warm and dry post-fire conditions that limit seedling establishment, promoting forest conversion to persistent non-forest states (Donato et al. 2016b, Stevens-Rumann et al. 2018, Davis et al. 2019, Kemp et al. 2019, Stevens-Rumann and Morgan 2019). In contrast, fire exclusion legacies are thought to have marginally affected the structure and composition of more mesic forests, like those in the mid-upper Cascades, where climate has naturally limited the ignition and spread of fire, except during periods of extreme climate

variability (Agee 1993, Krawchuk and Moritz 2011). Although high-severity fire in more mesic forests can create the same bottleneck of limited seed availability, greater moisture availability and reduced fire frequency can promote forest recovery, albeit over longer time spans (centuries instead of decades), reducing chances of large-scale forest conversion (Franklin and Hemstrom 1981, Agee 1993, Turner and Romme 1994).

Recent research on the impacts of high-severity and/ or short-interval fire (hereafter SIF; <25-yr interval; Donato et al. 2009b) on forest recovery has primarily been conducted in semi-arid environments (i.e., dry-warm or dry-cool; Fig. 1). Dry climate has historically facilitated frequent and low-to-mixed-severity fire regimes in these forests (Hessburg et al. 2019), resulting in sparse fuel density and connectivity and a higher proportion of conifer species with fire-adaptive traits and drought tolerance (e.g., Douglas fir [*P. menziesii*], ponderosa pine [*P. ponderosa*], and sometimes lodgepole pine [*P. contorta*]). Recent studies in the northern Sierra Nevada Range (Coppoletta et al. 2016), the Northern Rockies of central Idaho (Stevens-Rumann and Morgan 2016), the Bob Marshall Wilderness of Montana (Larson et al. 2013), and the Jemez mountains of New Mexico (Coop et al. 2016), among others, suggest that SIFs in relatively dry conifer forests lower woody fuel loads and post-fire conifer seedling densities. Considering the negative impacts fire exclusion legacies have had on forest resilience within these drier environments, it is clear that SIFs are part of the natural range of variation here (Hessburg et al. 2019). Thus, the reintroduction of SIFs into dry forests that have experienced fire exclusion, while challenging (e.g., Haugo et al. 2019), may increase long-term forest resilience by realigning forest structure with the more frequent but lower-severity fire disturbance patterns as prior to 20th-century fire exclusion (Larson et al. 2013, Stevens-Rumann and Morgan 2016).

Compared to the modest effects of most SIFs in semi-arid systems, two recent studies reported opposite and extreme impacts of high-severity fire and SIFs on forest recovery. In the wet and warm Klamath-Siskiyou coastal range, post-fire conifer regeneration was not substantially limited by high-severity fire and/or SIFs. Heterogeneous terrain and complex fire severity patterns

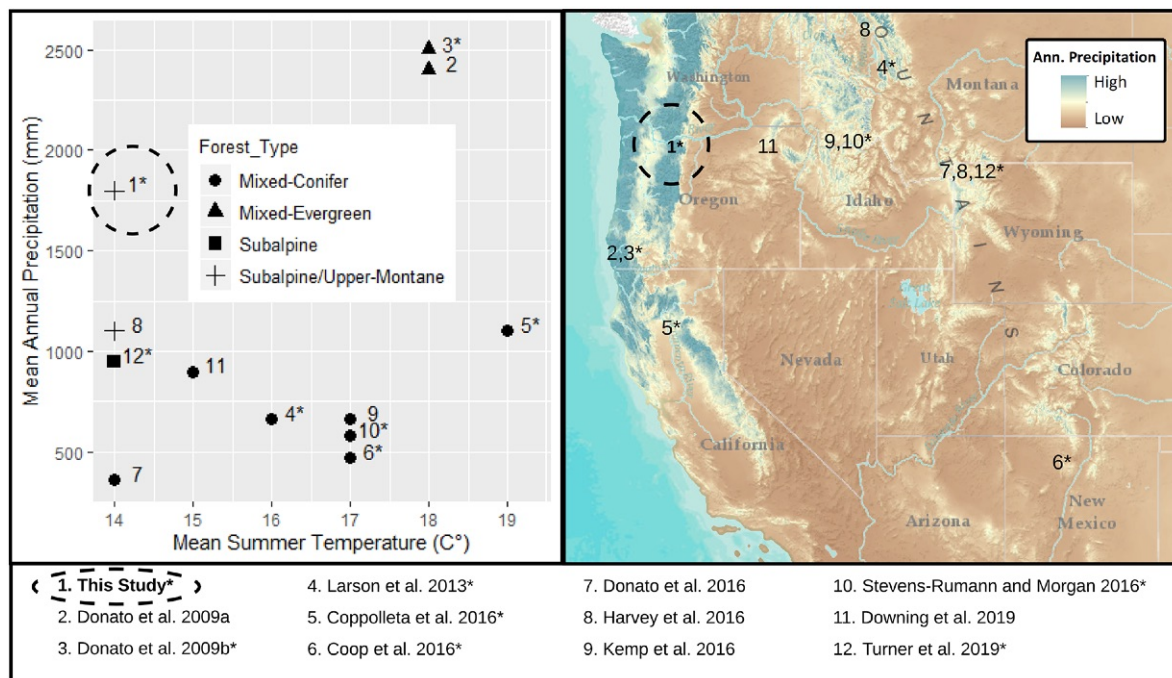


Fig. 1. Climatic and geographic distribution of recent studies in the western United States assessing temperate forest recovery after high-severity and/or short-interval fires (SIFs, marked by an asterisk). Mean climate estimates were extracted from each geographic study area using the ClimateWNA dataset (800 m spatial resolution; Wang et al. 2016); estimates are recent normal conditions (2000–2015).

provided sufficient proximate live seed sources and climate provided ideal moisture availability (Donato et al. 2009a, b). Although the Klamath-Siskiyou region experiences relatively hot summer conditions, mean annual precipitation can reach over 4000 mm (Donato et al. 2009a). Alternatively, in the cool, dry, inland subalpine forests of Yellowstone National Park, high-severity SIFs caused a sixfold reduction in post-fire seedling recruitment of serotinous lodgepole pine (*P. contorta* var. *latifolia*) when compared to a single high-severity fire (Turner et al. 2019). These results support concerns over the erosion of serotinous plant resilience in the face of SIFs, for which fire-return interval is shorter than seed production cycle (Buma et al. 2013, Enright et al. 2015). Although observed reductions in post-fire seedling densities following SIFs in this study were substantial, they were not indicative of causing non-forest or alternate forest state transitions (Turner et al. 2019). These recent studies add important new evidence of variability in conifer forest resilience to changing fire regimes

in specific bioclimatic conditions, and yet high-severity and SIF impacts on climatically cool and wet conifer forests, like those in the Cascade Range, have yet to be evaluated.

Within mid-to-high-elevation forest zones (>1000 m) in the Central Cascade Range in the PNW, several spatially large, severe, SIFs have occurred since 2000, aligning with observed increases in forest fuel aridity across the continental western United States (Abatzoglou and Williams 2016). These SIFs have primarily occurred around two large volcanic landscape features on the eastern edge of the High Cascades, Mt. Adams, Washington (WA), and Mt. Jefferson, Oregon (OR; see Appendix S1: Fig. S1 for photo representation). With historically wet and cool climate limiting fire frequency in these environments to an expected 50–200 + yr return interval (LANDFIRE 2010, Stine et al. 2014), the possible compound impact of high-severity fire and substantially increased fire frequency (7–11-yr interval) on forest recovery are presently unknown. In this study, we empirically

evaluated the hypothesis that increased, novel fire activity may disrupt the recovery of forests dominated by shade-tolerant species in the upper-montane and subalpine zones of the Central Cascade Range. Beyond the Cascade Range, our results may inform hypotheses on regeneration of shade-tolerant obligate seeding conifers following high-severity fire and SIFs in cool and/or moist forests elsewhere. We specifically asked the following questions to explore components of this hypothesis:

1. How does post-fire forest structure contrast between stands exposed to recent SIFs and those burned only once?
2. How do slope microclimate (aspect), fire severity and frequency, post-fire remnant forest structure, and post-fire climate conditions relate to conifer regeneration?
3. How does the order of burn severity in SIFs, low-then-high vs. high-then-low severity, influence conifer seedling abundance and composition?
4. Do large distances to seed sources, due to large fire perimeters of severe fires, favor forest state transitions at the patch level?

METHODS

Study areas

The fires in this study were in mid-to-high-elevation upper-montane and subalpine forests on two volcanic mountains of the Central Cascade Range of the PNW, Mt. Adams, WA, and Mt. Jefferson, OR (Fig. 2). The study areas were located between 1215 and 1650 m in elevation amid humid Mediterranean conditions, with total annual average precipitation ranging from 1700 to 2300 mm at Mt. Adams and 1600 to 2000 mm at Mt. Jefferson (PRISM 2018; 1981–2010 means; 800 × 800 m spatial resolution). Typically, winter precipitation is as snow above 1000 m elevation. At Mt. Adams, average temperatures range from -5° to 1°C in January and from 8° to 21°C in July (PRISM 2018). Due to a slightly more southern and eastern position, burned areas were slightly warmer at Mt. Jefferson, with average temperatures -4° – 3°C in January and 6° – 25°C in July (PRISM 2018). Although both Cascade landscapes receive substantial annual precipitation,

the sites studied were slightly toward the eastern margin of the Cascade Range and therefore climatically drier than some west Cascade mountain forests (Franklin and Dyrness 1973). Mts. Adams and Jefferson are part of the younger geologic High Cascade Range. Soils in these landscapes are dominantly well draining, ashy sandy loam andisols (Hildreth 2007, USDA 2018).

Forests on these Central Cascades landscapes are generally defined as upper-montane at ~1215 m elevation, mixed ~1350 m, and characteristically subalpine above ~1450 m (Franklin and Dyrness 1973; Appendix S1: Tables S1, S2). True firs were the dominant conifer species across the study areas, with grand fir (*A. grandis*) in the upper-montane and subalpine fir (*A. lasiocarpa*) in the subalpine. Ponderosa pine (*P. ponderosa*) and lodgepole pine (*P. contorta*) are the primary shade-intolerant species. Both the non-serotinous (var. *murrayana*) and serotinous (var. *latifolia*) subspecies of *P. contorta* are understood to be present within the Central Cascade Range (Atzet and McCrimmon 1990). The expression of serotiny by *P. contorta* in the Cascade Range is poorly understood, but studies elsewhere have linked serotinous cone production to environment, tree age, and fire history (Lotan and Perry 1983, Schoennagel et al. 2003).

Historic fire-return intervals are thought to have ranged from 50 to 200 + yr in our study areas, with fire frequency increasing at lower elevations (LANDFIRE 2010, Stine et al. 2014); dendrochronological studies of fire regimes have not been conducted here. Native Americans frequently set fire in lower-elevation forests in the Cascade Range for maintaining hunting and foraging grounds and in higher elevation forest to promote huckleberry growth; intentional subalpine burning may have been limited in extent and/or concentrated around trails, however (Boyd 1999, Steen-Adams et al. 2019). Since the early 20th century, the western halves of Mt. Adams and Mt. Jefferson have been owned and managed by the U.S. Forest Service and the eastern halves managed by the Confederated Tribes of the Yakima and Warm Springs Nations, respectively. Over the late 19th and 20th centuries, common forest management practices such as fire suppression, logging, and grazing have occurred on the western halves of these landscapes and, more recently, also on the

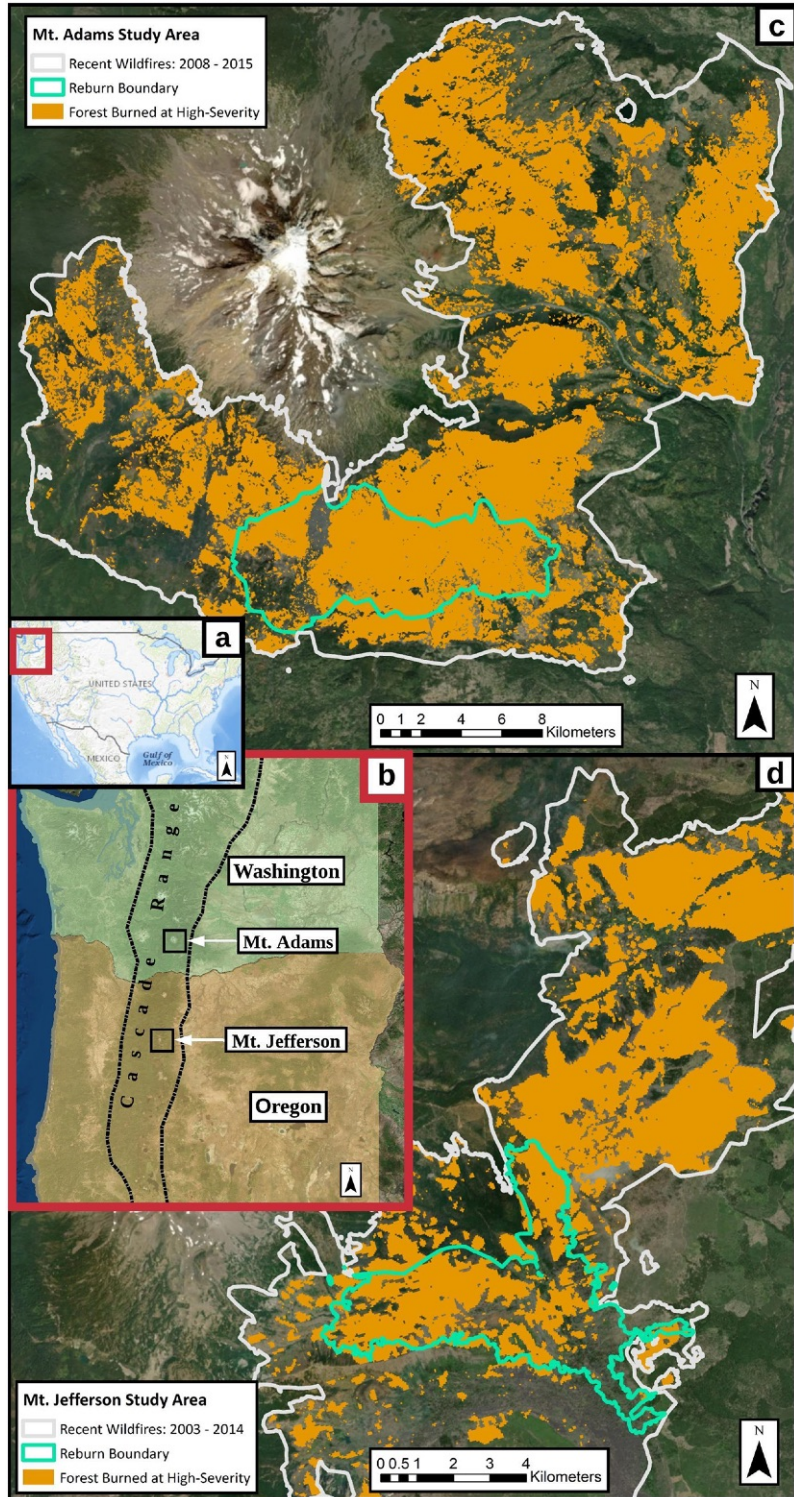


Fig. 2. Location of the study areas on (a) map of the continental United States and (b) the Oregon and Washington Cascades, (c, d) sampled wildfire perimeters, reburned areas, and extents of high-severity fire effects for the Mt. Adams and Mt. Jefferson study areas.

eastern halves. Most management legacies have been concentrated at elevations lower than our study areas, however.

Between 2003 and 2015, forests in our study areas have burned expansively, severely, and repeatedly. On Mt. Adams, these wildfires include the 2008 Cold Springs, 2012 Cascade Creek, and 2015 Cougar Creek fires (~30,000 cumulative ha burned; Fig. 2). On Mt. Jefferson, the wildfires include the 2003 Booth and Bear Butte (B&B) Complex, 2007 Warm Springs Area (WSA) Lightning Complex, and 2014 Bear Butte 2 fires (~39,000 cumulative ha burned; Fig. 2). All fires were caused by lightning and started burning between mid-July and early September. For the areas we sampled in the summer of 2018, time since fire ranged from three to fifteen years and the interval between repeated fires (SIFs) was either seven years (Cold Springs and Cougar Creek; WSA and Bear Butte 2) or eleven years (B&B Complex and Bear Butte 2).

Sampling design

To focus on natural post-fire forest regeneration, areas that experienced recent management influence (logging, post-fire salvage logging, and replanting) were excluded using documentation from associated land management entities. Areas with undocumented management efforts were detected and excluded via detailed visual interpretation of recent satellite imagery (2017). Additionally, potential sampling areas were set back a minimum distance of 100 m from roadways.

In the PNW, several insect species affecting conifers are known for large-scale outbreaks, which can lower tree resilience to future disturbance or cause outright mortality (Hummel and Agee 2003, Raffa et al. 2008, Meigs et al. 2015b). Two specific native insect species have been documented as significantly affecting mid-to-high-elevation upper-montane and subalpine forests in the Cascade Range: Western Spruce Budworm (WSB) and Mountain Pine Beetle (MPB; Meigs et al. 2015a). Although insect-affected forest stands are not necessarily more likely to burn than their unaffected counterparts, weakened or killed trees likely alter fire dynamics like burn severity, fire temperature and spread, biomass consumption, and possibly post-fire tree regeneration (Harvey et al. 2014, Meigs et al. 2015b). Meigs and colleagues mapped cumulative tree

mortality from MPB and WSB outbreaks (in units of dead tree basal area per hectare, DTBA; $m^2 ha^{-1}$) by combining Aerial Detection Survey (ADS) data 1970–2012 and Landsat satellite imagery (LT) 1984–2012 across the PNW region (Meigs et al. 2015a). In the Mt. Adams and Mt. Jefferson vicinity, areas with insect-caused tree mortality values beyond 3.0 (cumulative) DTBA per WSB and/ or MPB activity, or roughly >5% of the maximum DTBA value observed in the dataset, were removed from further analyses. Our rationale for these thresholds was a compromise between minimizing insect effects on regeneration dynamics and having enough area available to sample (as relatively little area existed with 0 DTBA $m^2 ha^{-1}$; Meigs et al. 2015a).

Fire perimeters and burn severities were obtained for our study areas from the Monitoring Trends in Burn Severity (MTBS) program, which has mapped burn severity of large (>400 ha) wildland fires in the United States since 1984 at 30-m resolution using Landsat satellite imagery products (Eidenshink et al. 2007). We identified burn severity in our study areas using the relativized delta normalized burn ratio (RdNBR), which was classified into discrete burn severity groups following the spectral value thresholds outlined by Miller and Thode (2007). We specifically retained low- and high-severity classes for stratification purposes. Forests burned at moderate severity likely have their own unique post-fire dynamics, but their conditions can be difficult to validate in the field and thus were excluded from our analyses (e.g., after Stevens-Rumann and Morgan 2016). To assess the effect of wildfire on regeneration dynamics, our burn stratification design considered single burn (control) vs. SIFs with reburn at low and high burn severities, as well as the sequence of burn severity (low-high vs. high-low), which reportedly differs in effect on post-fire conifer regeneration dynamics (Stevens-Rumann and Morgan 2016). A smaller number of unburned sites, located immediately outside of wildfire perimeters, were also included to represent stand structure conditions of local forests in the absence of recent wildfire. Finally, to ensure and increase the accuracy of remote-sensing methods described above to delineate fire perimeters, potential sampling areas were buffered 100 m from all fire-perimeter boundaries.

To quantify the effect of long-term moisture availability on post-fire regeneration, plot location was additionally stratified by Heat Load Index (HLI; McCune and Keon 2002). HLI was derived from a 30-m digital elevation model (DEM). HLI values range between zero and one: In the Northern Hemisphere, values closer to zero represent wet/cool conditions (northeast-facing aspect) and values closer to one represent dry/warm conditions (southwest-facing aspect). To contrast relatively wet- and dry-aspect sites, areas with values in the top and bottom 25th percentiles were retained for stratification purposes. These 25th percentile wet and dry classes were then geographically overlaid upon burn classes described above to produce the final field sampling stratification, represented as strata delineation polygons within the study areas (Table 1).

Field-plot coordinates within strata delineation polygons were generated using a stratified random selection. During the plot generation process, all potential sample plots in each study area were buffered a minimum distance of 100 m from each other to minimize spatial autocorrelation (mean distance between plots was 4083 m; range 110–13,048 m). Additionally, to maintain uniformity and avoid misclassifications of stratified field conditions (i.e., burn severity and slope aspect; HLI), each sample plot was restricted to a contiguous-strata delineation polygon of one hectare or greater in size. We generated eight random plot locations per stratum, plus four random unburned plot locations for each study area. This final selection procedure resulted in a total target of $n = 72$ plots per study area, or $n = 144$ plots total. We physically sampled only 122 plots of this total selection during the summer of 2018

due to field season constraints (Table 1; and see Appendix S1: Fig S2). Due to the expansive, contiguous nature of the wildfires on Mt. Adams making unburned forest rare, and access issues due to extreme topography on Mt. Jefferson, our unburned plots are relatively spatially clustered. Thus, our unburned plots may not capture the full range of forest structure heterogeneity in these study areas.

Data collection

Field data collection occurred during June–September of 2018. The preselected plots were accessed by hiking from the nearest accessible road. Once reached, each plot was field-verified for its membership in the designated burn severity and slope aspect (HLI) strata. Field burn severity was validated using evidence of ecological markers outlined by Key and Benson (2006) and simplified canopy tree mortality thresholds outlined by Whittier and Gray (2016). Low burn severity was field-verified by evidence of surface fire, including limited but present scorching of tree boles, minor removal of fine woody debris and organic soil, and <50% tree canopy mortality within plot. High burn severity was field-verified by tree canopy mortality >90%, significant bole charring, and significant removal of organic soils within plots. While we were not aware of guidelines for verifying SIF field conditions, reburns' effects on forest structure typically differed from fire evidence in single high-severity fire plots, including observations of increased bole charring and consumption of standing tree biomass, removal of fine woody debris, and increased soil charring at SIF plots. If the predetermined plot location did not meet anticipated criteria, the plot

Table 1. Field sampling stratification design.

Wildfire treatment	Burn severity	Slope microclimate (aspect)	Strataabbr.	Target sample size ($n =$ plots)	Achieved sample size ($n =$ plots)
Single recent wildfire	Low	Wet	LW	16	14
Single recent wildfire	Low	Dry	LD	16	14
Single recent wildfire	High	Wet	HW	16	13
Single recent wildfire	High	Dry	HD	16	13
Short-interval fire	Low-High	Wet	LHW	16	14
Short-interval fire	High-Low	Wet	HLW	16	14
Short-interval fire	Low-High	Dry	LHD	16	15
Short-interval fire	High-Low	Dry	HLD	16	14
Recently unburned	Unburned	Wet	UW	8	5
Recently unburned	Unburned	Dry	UD	8	6

location was moved within the immediate patch in 30-m intervals in a random cardinal direction until conditions correctly matched the designated strata (Stevens-Rumann and Morgan 2016; see Appendix S1: Table S3).

Data on physical site characteristics, pre-fire forest structure, post-fire conifer regeneration, post-fire ground and canopy cover, and abundance of down woody debris were recorded at each sample plot location in a 30 m diameter circular plot (0.07 ha; see Appendix S1: Fig. S3 for plot sampling diagram). Aspect, elevation, and slope were recorded at plot center using a compass and GPS. Within each plot, pre-fire stand structure was estimated by recording diameter at breast height (dbh) and status (live or dead, standing or uprooted) of all trees, with trees taken to be woody stems of >7.8 cm dbh (dbh at 1.37 m above ground level; Stevens-Rumann and Morgan 2016). We were able to identify dead trees at the species level following single burns given our study's relatively low tree species richness and the species' unique differences in remnant bark, stem, and branch structures. Although bark quickly falls from dead trees post-fire, remnant bark at the base of trees was very common in our study sites; we acknowledge, however, that some misidentification may have occurred, especially for SIF plots. Species-level identification after reburns was generally difficult due to substantial loss of identifying markers, so we excluded SIF plots from an analysis requiring pre-fire species-level information. To determine whether fire treatment affected woody stem charring and biomass loss, substantial stem charring ($>50\%$ of non-bark woody surface area) was recorded as presence/absence on a per-tree basis and then reported as mean tree charring (percentage of trees) at the plot level.

Post-fire conifer seedlings were counted within four variable-width belt transects, which were set facing cardinal directions (i.e., perpendicular to each other). Belt-transect width varied depending on seedling densities (Harvey et al. 2016, Donato et al. 2016b), but default size for each was 2×15 m (0.012 ha total). When the number of estimated seedlings was above 200 or below 10 individuals inside the default transects, belt-transect size was reduced to four 0.5×15 m (0.003 ha) belt transects or increased to the entire circular plot (0.07 ha), respectively.

For each seedling, we recorded species and approximate age by bud-scar count (Urza and Sibold 2013, Hankin et al. 2018). Bud-scar counts were used to determine whether seedlings established pre-fire, post-fire, or post-reburn.

To estimate down woody debris at the sampling sites, four 14 m length transects were run in cardinal directions from plot center. Coarse (>7.62 cm diameter, 1000 hr fuel) and intermediate-and-fine (combined, <7.62 cm diameter, 1–100 hr fuel) woody fuels were separately tallied every 1 m along transect lines following the planar intersect method outlined by Brown (1974). Similar to trees, each individual log or branch of coarse woody debris (CWD) was tallied for the presence of substantial charring ($>50\%$ woody surface area) and reported as mean CWD charring (%) at the plot level. Percent ground cover by shrubs, forbs, grasses, litter/duff, and bare soil/rock was visually estimated to the nearest 5% within five 2×1 m quadrats (0.001 ha), one located at plot center and the remaining four placed at 7 m from plot center each along the four cardinal direction transects. The average of the five quadrats was reported as mean ground cover (percentage of area) at plot level. Remnant canopy cover (%) was measured using a spherical densiometer at ~ 1.3 m from ground at the same five locations as ground cover quadrats. Canopy cover was recorded facing each cardinal direction, averaged for each sample location, and then averaged among the five quadrat locations to represent plot-level conditions. Finally, horizontal distance from plot center to the ten nearest, live, seed-bearing conifer trees was recorded using a rangefinder (TruPulse 200/Laser Technology). If these trees were located >500 m from plot center, they were tallied and reported as a distance >500 m category (Kemp et al. 2016).

Statistical analysis

All statistical analyses were completed in R version 3.5.2 (R Core Team 2017) using standard core packages, unless otherwise noted below.

Post-fire forest structure

To identify potential differences in post-fire forest structure among sampled fire treatments across the study areas, referred to hereafter as unburned (U), low (L), high (H), low-then-high (LH), and high-then-low (HL) burn severity

treatments, univariate and multivariate methods were utilized following Stevens-Rumann and Morgan (2016). For both univariate and multivariate analyses, post-fire forest structure was summarized by twelve field-measured variables: live tree density, percent charred dead trees, distance to seed source, percent canopy cover, coarse and fine down woody debris abundance, percent charred coarse woody debris, and percent ground cover (litter/duff layer, bare soil/rock, grass, shrub, and forb). Nonparametric statistical methods were used due to non-normal distributions and unequal variance in the data and unequal sample sizes among fire treatments.

To detect potential differences in individual forest structure variables among fire treatments, the Kruskal-Wallis test was used to assess for statistical differences in the univariate analysis. When differences were detected, a Games-Howell post hoc test (appropriate for unequal sample sizes) was used for pairwise comparisons utilizing the userfriendlyscience R package (Peters 2018). Resulting p-values were adjusted using the Holm method to correct for increased type I error by multiple pairwise comparisons (Aickin and Gensler 1996). For the multivariate analysis of stand structure, a permutational multivariate analysis of variance (PERMANOVA) was used in R via the vegan R package (Oksanen et al. 2018). For our analysis, number of permutations was set to 999 and dissimilarity measure to Bray-Curtis distance (Anderson 2017). As for the univariate analysis, we also used the Holm method to adjust p-values for multiple pairwise comparisons. Finally, a non-metric multidimensional scaling (NMDS) ordination plot was developed to aid in visual interpretation of results, using the vegan and ggplot2 R packages (Wickham 2016, Oksanen et al. 2018).

Pre- and post-fire forest density and composition

To evaluate potential shifts in forest composition and investigate impacts of slope microclimate (aspect) and fire treatment on seedling establishment, several analyses were conducted. Pre-fire (tree) and post-fire (seedling) species composition, calculated as mean percent of plot density (i.e., number of stems/ha) among plot groupings, was compared across slope aspect (HLI) and fire treatments. For pre-fire composition, SIF plots (LH and HL) were excluded from

calculations due to substantial biomass loss and difficulties in species identification. With all species combined, pre-fire tree density was compared across slope aspects (HLI), while post-fire seedling density was compared across slope aspects (HLI) and fire treatments. For tree and seedling density, the Kruskal-Wallis test and Games-Howell post hoc test (when differences were detected) were used to test for significant differences between groups. For multiple pairwise comparisons, the Holm method was used to pre-adjust resulting *P*-values.

To aid in visualizing and interpreting seedling composition results across fire treatments, an NMDS ordination was generated to represent post-fire seedling abundance by species. Recently burned plots ($n = 111$) with no seedlings detected ($n = 21$) were removed from the analysis as required. Bray-Curtis distance was used and NMDS solutions were tried in second and third dimensions; we chose to use fewer dimensions when stress score differences were marginal between second and third dimensions (<0.05). The vegan and ggplot2 R packages were used to generate NMDS plot figures (Wickham 2016, Oksanen et al. 2018). Finally, to determine temporal patterns of seedling establishment in SIF plots (LH and HL), we classified and quantified the percentage of post-fire seedlings that established after the first and second fires using bud-scar estimates.

Drivers of post-fire seedling abundance

To identify factors influencing conifer regeneration, the abundance of post-fire conifer seedlings was modeled as a function of post-fire ecological legacies (distance to seed source, remnant canopy cover, and CWD, bare soil, or shrub cover; see Table 2), abiotic environmental conditions (elevation, slope, heat load index [HLI], topographic wetness index [TWI]), time (since a high-severity fire occurred), and post-fire climate conditions (spring snow water equivalent and mean summer temperature in first three years after a high-severity fire). Although sampling was stratified only by slope microclimate (i.e., by HLI, a variant on slope aspect), two different measures of hillslope microclimate and moisture availability were tested in the seedling regeneration models: heat load index (HLI; i.e., transformed of slope aspect, related to solar radiation

and evapotranspiration potential; McCune and Keon 2002) and topographic wetness index (TWI, a proxy for likely soil moisture based on the convergence and divergence of terrain; Beven and Kirkby 1979). Since the distribution of seedling density data was strongly right-skewed, with unequal variance and over-dispersed, individual seedling species were grouped into two broad functional groups defined by shade tolerance to minimize the number of zeros and improve model fit (Zuur et al. 2012). Shade tolerance was assigned to each conifer species based on the USFS Fire Effects Information System (FEIS; Abrahamson 2018) with *Abies*, *Picea*, *Tsuga* spp. broadly classified as shade-tolerant and *Psudotsuga*, *Pinus*, *Larix* spp. classified as shade-intolerant (see Appendix S1: Table S2).

Generalized linear models (GLM) with a negative binomial distribution (logit-link) were developed for predicting seedling counts using the MASS R package (Venables and Ripley 2002) following Kemp et al. (2016). Three distinct count

models were developed in total using all burned plots ($n = 111$): for all species combined, for shade-tolerant species only (*Abies*, *Picea*, *Tsuga*), and for shade-intolerant species only (*Psudotsuga*, *Pinus*, *Larix*). All variables from Table 2 were included in preliminary fitted models prior to model simplification. To account for the variable transect sizes used for seedling counts (0.003, 0.0120, and 0.0706 ha), an offset variable was included within model equations (Zuur et al. 2012, Kemp et al. 2016). Upon fitting a full model, outlier data points were assessed using Cook's distance when plotting Pearson's residuals against fitted values. Significant outliers, indicated as having Cook's distance >0.5 , were removed from each model to improve performance and meet assumptions (Cook 1979). Full models ($n = 109$; two outliers removed) were then simplified to include only significant variables ($P < 0.05$) using a backward stepwise procedure in which each variable was assessed simultaneously for model improvement through

Table 2. Predictor variables included in post-fire seedling regeneration models and their methods of measurement.

Category	Variable	Method of measurement	Units	Type	Range
Fire legacies	Distance to live seed source	Field measured (10 closest mature trees; averaged)	m	Continuous	Bounded [15 500]
	Coarse woody debris	Field measured (abundance)	Integer	Continuous	Bounded [0 56]
	Canopy cover	Field measured (5 plots, averaged)	%	Continuous	Bounded [0 100]
	Bare soil cover	Field measured (5 plots, averaged)	%	Continuous	Bounded [0 100]
	Shrub cover	Field measured (5 plots, averaged)	%	Continuous	Bounded [0 100]
Abiotic	Elevation	Field measured	m	Continuous	Bounded [1215 1650]
	Slope	Field measured	Degrees	Continuous	Bounded [5 40]
	Heat load index (HLI)	Derived from field-measured slope, aspect, and latitude (McCune and Keon 2002)	Unitless	Continuous	Not bounded [0.38 1.01]
	Topographic wetness index (TWI)	Derived from a 30 m DEM; ArcGIS (Beven and Kirkby 1979)	Unitless	Continuous	Not bounded [5.67 14.27]
Time	Time since a high-severity fire	Year of sampling (2018) minus year of high-severity burn	Years	Continuous	Discrete values [3,4,6,10,11,15]
Post-fire climate	Spring snow water equivalent (SWE)	March–May averaged SWE (deviation from 15-year normal) 0–3 yr after a high-severity fire (SnoDAS; SnoDAS 2004)	mm	Continuous	Not bounded [−534.16 350.14]
	Mean summer temperature (MST)	June–September averaged MST (deviation from 30-year normal) 0–3 yr after a high-severity fire (METDATA; Abatzoglou 2013)	°C	Continuous	Not bounded [0.01 0.18]

its removal using absolute decreases in AIC_c and chi-square probability (Zuur et al. 2012). Multicollinearity was assessed in the original (full) and final (simplified) models using the variance inflation factor (VIF) measure. The final set of explanatory variables used displayed VIF values <2.0, indicating minor collinearity detected (Zuur et al. 2010). In addition to visual assessment of model residuals against fitted values, a Pearson's chi-squared test was performed to assess each model's goodness of fit (Zuur et al. 2012). Prediction performance was evaluated by comparing predicted and observed values from each model using Spearman's rank correlation (ρ ; Kemp et al. 2016).

To illustrate the impact of seed source availability on post-fire seedling abundance, the three final GLM models (Shade-Tolerant, Shade-Intolerant, and All Species) were used to plot model realizations of seedling abundance as a function of increasing distance to seed source (just one of the component variables of the models). To include but reduce the influence of model parameters other than distance to seed source in each probability curve, parameters in each GLM model were kept at their median value for all burned plots when generating the plotted realizations of seedling probability curves following Kemp et al. (2016).

Future forest trajectories: plot to patch scale

To explore future forest trajectories of severely burned forest and relate plot-scale results to the forest patch-scale and across landscapes, the following procedures were conducted. First, within the full extent of the large wildfire perimeters around our study areas, distances were calculated from forest patches burned at a high-severity to those with assumed live seed source (unburned or burned at low or moderate severity; Kemp et al. 2016). To do this, using classified MTBS burn severity (RdNBR) raster datasets within each wildfire perimeter in ArcGIS, area burned at a high-severity during an initial wildfire and/or reburn was extracted and joined into a single raster layer. All other area that did not burn at a high-severity during any fire event was similarly extracted and joined into a separate layer. These two raster layers were then converted to point features, and the Near ArcGIS tool was used to compute the shortest Euclidean

distance from each high-severity point to a point with assumed live seed source. Due to the spatial resolution of the raster imagery (30 m), the minimum distance measured from a high-severity point to lower-severity point was 30 m. Subsequent statistics were computed in R using the distances table exported from ArcGIS.

Finally, three future forest trajectory pathways were developed based on anticipated future fire frequency, the sampled pre-fire forest density of our study areas, and conservative mixed-conifer forest restocking thresholds used by Stevens-Rumann and Morgan (2016). Our three forest trajectories are defined as non-forest (<100 seedlings/ha), low-density forest (100–250 seedlings/ha), and recovered forest (>250 seedlings/ha). Modeled seedling abundance as a function of distance to seed source (all species model) was utilized to classify percentages of the broader study areas that were burned at a high-severity that would likely fall into each of these three forest trajectory pathways, based on their computed distance to live seed source. We acknowledge that due to the spatial resolution of our remotely sensed burn severity data (30 m), projecting fine-scale patterns of regeneration to the landscape scale involves an inherent degree of error. Thus, some fine-scale patterns may be more nuanced than our analysis can capture.

RESULTS

Fire effects on forest structure

The post-fire forest structure of low-severity (L), unburned (U), high-severity (H), and SIF (LH and HL) forest plots differed significantly overall among our central Cascades mesic, mixed-conifer forest study areas (see Appendix S1: Figs. S4 for photo representation and S5 for NMDS ordination, Table S4 for PERMANOVA results). Cumulative post-fire forest structure (across twelve characterizing variables, Table 3) was significantly different between single-burned and SIF fire treatments ($P = 0.001$), though SIF treatments with different burn order (high-then-low HL and low-then-high LH) did not structurally differ ($P = 0.263$), nor did U and L plots ($P = 0.263$). Plots that experienced only a single high-severity fire (H) were structurally distinct from plots of the other fire treatments ($P = 0.001$).

After a reburn event, distance to live seed source and proportion of charred trees (%) at

Table 3. Median \pm SE (IQR) forest structure characteristics across sampled fire treatments.

Forest structure characteristics unburned	Burned once		SIF reburned		
	(U, n = 11)	Low severity (L, n = 28)	High severity (H, n = 26)	Low-High (LH, n = 29)	High-Low (HL, n = 28)
Standing canopy					
Live tree density (trees/ha ⁻¹)	297 ^a \pm 60 (142–460)	269 ^a \pm 28 (205–354)	0 ^b \pm 0 (0–0)	0 ^b \pm 0 (0–0)	0 ^b \pm 0 (0–0)
Distance to seed source (m)	15 ^a \pm 0 (15–15)	15 ^a \pm 0 (15–15)	54 ^b \pm 25.4 (19–148)	180 ^c \pm 27.5 (133–330)	199 ^c \pm 30.9 (106–364)
Charred trees (%)	0 ^a \pm 0 (0–0)	1.9 ^b \pm 0.5 (0–3.7)	17.0 ^c \pm 4.6 (5.4–48.0)	74.2 ^d \pm 5.4 (35.7–88.4)	53.3 ^d \pm 5.2 (32.7–76.8)
Remnant tree canopy cover (%)	85 ^a \pm 2.3 (67–87)	83 ^a \pm 1.4 (76.5–86.0)	29.5 ^b \pm 3.1 (23–46)	31 ^b \pm 2.6 (21–36)	15 ^c \pm 1.8 (8.5–21.5)
Ground cover					
Bare soil/rock (%)	4 ^a \pm 2.2 (0–5)	0 ^a \pm 1.8 (0–5)	56 ^b \pm 3.7 (45–70)	70 ^b \pm 2.7 (60–77)	51.5 ^b \pm 4.9 (30–70)
Litter/duff (%)	61 ^a \pm 8.4 (27.5–71)	57.5 ^a \pm 4.6 (49.5–78)	0 ^b \pm 0 (0–0)	0 ^b \pm 0 (0–0)	0 ^b \pm 0 (0–0)
Grass (%)	1 ^a \pm 2.7 (0–4.5)	0.5 ^a \pm 1.8 (0–11.5)	3 ^a \pm 3.1 (0–23)	0 ^a \pm 2.4 (0–11)	6 ^a \pm 4.7 (0–44.5)
Forb (%)	9 ^a \pm 4.2 (4.5–29)	9.5 ^a \pm 3.1 (3–22)	7 ^a \pm 1.7 (1–15)	4 ^a \pm 1.8 (2–9)	5.5 ^a \pm 1.5 (3–9)
Shrub (%)	18 ^a \pm 3.9 (5–29)	5 ^a \pm 1.8 (1.5–13.5)	1 ^a \pm 3.9 (0–9)	3 ^a \pm 2.5 (0–14)	5 ^a \pm 2.4 (0–18)
Down woody fuels					
Fine fuels \leq 100h (count)	33 ^a \pm 2 (28.5–38.5)	30.5 ^a \pm 1.4 (28–38)	17 ^b \pm 1.7 (12–25)	9 ^c \pm 1.4 (5–14)	9 ^c \pm 1.1 (6–13.5)
Coarse fuels 1000 + h (count)	8 ^{a,b} \pm 0.8 (5–9.5)	4 ^a \pm 0.5 (2.5–6)	5 ^{a,b} \pm 0.6 (3–7)	4 ^a \pm 0.5 (2–6)	8.5 ^b \pm 0.6 (5.5–10)
Charred coarse fuels (%)	0 \pm 0 ^a (0–0)	25 ^b \pm 7 (0–58.3)	42.8 ^{b,c} \pm 7.6 (25–100)	100 ^c \pm 4.5 (100–100)	68.3 ^c \pm 5.5 (47.2–88.8)

Notes: Different superscripted letters indicate significant pairwise comparisons in fire treatment differences for a given forest characteristic (i.e., univariate analysis, across rows). Pairwise comparisons were performed using Games-Howell post hoc test when significant differences were detected from Kruskal-Wallis test. The Holm adjustment method was used to control for type 1 error among multiple pairwise comparison.

least tripled: Distance increased more than threefold for SIFs compared to H treatments (univariate analysis; Table 3). No mature live trees were present within plots that experienced any high-severity fire, either as an individual event or as part of a reburn sequence (H, LH, HL). Compared to L and U plots, only about 36% of remnant tree canopy cover remained within H and LH plots (albeit dead) and 18% in HL plots. For fine down woody fuels, H plots exhibited only about 52% the fine-fuel abundance, and HL plots 28% at the time of surveying (after the fires), compared to L or U plots. Abundance of groundcover vegetation groups (grasses, forbs, shrubs) as percent cover did not vary across treatments. Bare soil made up over 50% of ground cover across plots that experienced at least one high-severity fire (H, LH, HL).

Pre- and post-fire forest density and composition

We counted over 4200 adult trees (>7.8 cmdbh, standing or uprooted, i.e., pre-fire composition) and over 4000 seedlings (i.e., post-fire composition) of ten different conifer species across 122 plots stratified by fire treatments and slope microclimates (Table 4). Pre-fire tree densities were statistically greater ($P = 0.0001$) in plots in wet-aspect settings (low heat load index [HLI]) and included a larger proportion of shade-tolerant species than dry-aspect (high HLI) sites. Across all plots for which pre-fire tree species could be identified (i.e., all unburned or once-burned plots; $n = 65$), pre-fire tree composition was dominated (~20–35%) by *A. grandis* and *A. lasiocarpa*, with smaller components of *P. menziesii* and *P. ponderosa*.

Total seedling densities were consistently low across plots that had experienced any high-

Table 4. Median conifer density (IQR) and mean percent of plot density \pm SE by species composition (and shade tolerance⁺ or intolerance⁻) of pre-fire trees and post-fire established seedlings, stratified by wet/dry aspect and fire history (L, H, LH, HL).

Conifer density as median stems/ha (IQR)	Conifer species composition (mean % of plot density \pm SE)								
	<i>Pinus</i> <i>contorta</i> ⁻	<i>Pinus</i> <i>ponderosa</i> ⁻	<i>Pseudotsuga</i> <i>menziesii</i> ⁻	<i>Abies</i> <i>grandis</i> ⁺	<i>Abies</i> <i>lasiocarpa</i> ⁺	<i>Abies</i> <i>amabilis</i> ⁺	<i>Abies</i> <i>mertensiana</i> ⁺	<i>Tsuga</i> <i>mertensiana</i> ⁺	<i>Picea</i> <i>engelmannii</i> ⁺
Pre-fire trees									
All plots (<i>n</i> = 65)	566 (396–736)	4.7 \pm 1.1	10.2 \pm 3.0	11.2 \pm 2.5	34.8 \pm 3.9	24.0 \pm 4.0	4.5 \pm 1.6	6.0 \pm 1.7	3.7 \pm 1.1
Wet-aspect plots (<i>n</i> = 32)	658 (481–1033)	6.5 \pm 2.0	1.3 \pm 0.5	5.6 \pm 2.4	35.4 \pm 5.6	28.1 \pm 5.3	6.6 \pm 3.1	10.1 \pm 3.2	5.1 \pm 1.9
Dry-aspect plots (<i>n</i> = 33)	439 (311–609)	2.8 \pm 1.1	18.9 \pm 5.5	16.5 \pm 4.1	34.3 \pm 5.6	20.0 \pm 6.1	2.4 \pm 1.0	1.4 \pm 0.7	2.5 \pm 1.3
Post-fire seedlings									
All plots (<i>n</i> = 111)	78 (14–1232)	22.1 \pm 3.5	7.9 \pm 2.2	10.4 \pm 2.1	21.6 \pm 3.1	8.4 \pm 2.1	2.7 \pm 1.1	2.1 \pm 0.7	4.1 \pm 1.4
Wet-aspect plots (<i>n</i> = 55)	8 (2–100)	30.6 \pm 5.4	5.7 \pm 2.4	7.6 \pm 2.9	16.1 \pm 3.8	12.2 \pm 3.7	2.5 \pm 1.2	3.5 \pm 1.3	7.6 \pm 2.8
Dry-aspect plots (<i>n</i> = 56)	5 (0–79)	12.8 \pm 4.0	9.8 \pm 3.6	12.8 \pm 3.1	26.4 \pm 4.9	4.5 \pm 2.0	2.8 \pm 1.8	0.6 \pm 0.3	0.5 \pm 0.2
L-severity (<i>n</i> = 28)	11,515 (4822–23,569)	0.9 \pm 0.3	3.3 \pm 2.5	19.6 \pm 3.9	51.1 \pm 5.8	5.3 \pm 3.2	7.7 \pm 3.6	0.6 \pm 0.3	8.2 \pm 4.0
H-severity (<i>n</i> = 26)	49 (0–141)	37.0 \pm 8.5	4.2 \pm 2.6	10.4 \pm 4.6	7.2 \pm 3.2	15.8 \pm 6.4	3.3 \pm 2.4	3.8 \pm 2.0	1.6 \pm 0.9
LH severity (<i>n</i> = 29)	28 (0–127)	24.1 \pm 7.5	11.4 \pm 5.2	11.9 \pm 5.9	24.3 \pm 7.7	5.9 \pm 3.7	NP	NP	NP
HL severity (<i>n</i> = 28)	14 (0–162)	26.6 \pm 7.0	12.3 \pm 5.9	0.1 \pm 0.1	3.9 \pm 2.8	7.2 \pm 3.0	NP	4.0 \pm 1.7	6.6 \pm 3.8

Notes: Pre-fire tree density and pre-fire species composition were estimated from plots with unburned, low-, and high-severity fire treatments (*n* = 65); reburned plots were excluded due to difficulty in species identification after two fires. Unburned plots were excluded from post-fire seedling calculations. NP indicates that species was not present at any sampled site of the indicated treatment. Wet and dry sites were classified using a heat load index related to hillslope aspect (see *Sampling Design*).

severity fire (H, LH, HL; 49, 28, and 14 median seedlings per hectare, respectively, not significantly different) and three orders of magnitude lower than in plots that had experienced only one low-severity fire (L, median 11,515 seedlings/ha; $P = 0.001$; Table 4). We were unable to find any conifer seedling in 20 of the 83 sites (24%) that had experienced a high-severity fire or reburn (H, LH, or HL). These median values of seedling density among severely burned plots correspond to a relative density of ~0.1–0.4% observed within low-severity plots (11,515 seedlings/ha), and to ~2–9% of pre-fire mature tree density across all plots (i.e., 566 mature trees/ha; Table 4). In contrast to pre-fire mature tree density, overall post-fire seedling density was not statistically different between wet- and dry-aspect

settings across all burned plots ($P = 0.942$; *n* = 111). *Pinus contorta* and *A. grandis* were dominant among post-fire seedling composition, overall. When comparing pre-fire to post-fire composition (by species, as mean percent of plot density; Table 4), there was an almost fivefold increase in *P. contorta* after fire, entirely in plots that had burned at least once at high severity (H, LH, HL), and an almost threefold decrease in *A. lasiocarpa*, which was exacerbated at drier-aspect sites. Generally, *P. contorta* was the dominant seedling species after any single high-severity fire or rapid reburn (H, LH, or HL; Table 4).

Order of burn severity among SIF plots, that is, HL vs. LH, influenced both temporal patterns of seedling establishment and species composition. Based on bud-scar estimates of seedling age, in HL

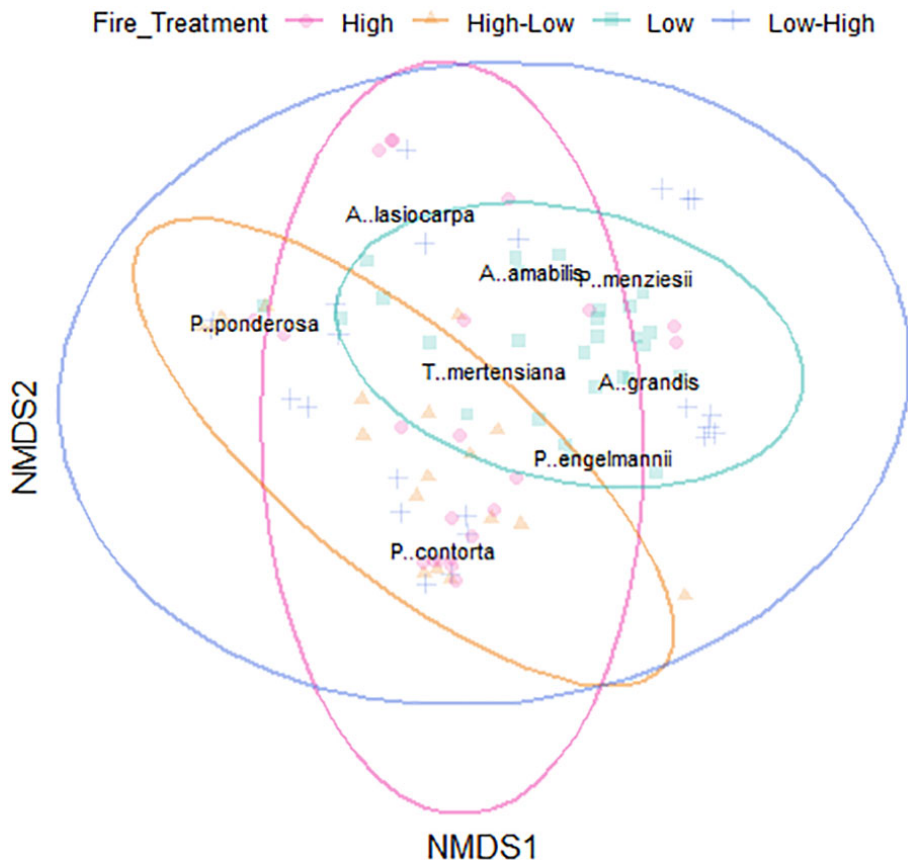


Fig. 3. NMDS ordination of post-fire seedling abundance, by species, among sampled fire treatments. Dissimilarities measured using Bray-Curtis distance; stress = 0.13, dimensions = 2. less coincident ellipses indicate more dissimilarity. Ellipses drawn using 95% confidence intervals. Sample size (n) among fire histories used in analysis: low (27), high (22), low-high (23), high-low (18). *P. monticola* and *L. occidentalis* seedlings were excluded from this analysis due to their low observed abundance (<1% seedlings).

plots, 72% of presently observed seedlings established after the first (H) fire and 28% after the second (L) fire. Instead, in LH plots only 0.2% of presently observed seedlings established after the first fire (L) and 99.8% after the second fire (H). Species post-fire composition results and the NMDS ordination revealed that a LH reburn appeared to support the establishment of all local conifer species, whereas a HL reburn preferentially supported *P. contorta* and *P. ponderosa*, despite the pines having a lower density prior to the initial fire in comparison with both *Abies* spp. (Fig. 3; Table 4).

Drivers of post-fire seedling abundance

Post-fire seedling abundance, overall, was most strongly predicted by remnant canopy cover, distance to seed source, and post-fire

spring snow water equivalent (SWE) across all species and burned plots combined (GLM results; Table 5). For shade-tolerant species (*Abies*, *Picea*, *Tsuga* genera), abundant canopy cover, short distance to seed source, low post-fire mean summer temperature (MST), and low SWE were the most important predictors of seedling abundance. In contrast, for shade-intolerant species (*Psudotsuga*, *Pinus*, *Larix* genera), low SWE, low fraction of bare soil cover, low fraction of shrub cover, and short distance to seed source (but more weakly than the shade-tolerant species) were the best predictors of seedling abundance (Table 5). Notably, time since a high-severity fire (3–15 yr) was not influential for either shade grouping nor overall. Count models passed model fit validation, as indicated by P

Table 5. Negative binomial GLM coefficient estimates (β), in log scale, for the final reduced seedling count models.

Predictors	All seedlings	Shade-tolerant	Shade-intolerant
Canopy cover (%)	0.025***	0.043***	...
Distance to seed source (m)	-0.018***	-0.038***	-0.025**
Post-fire spring snow water equivalent (SWE)	-0.009**	-0.022***	-0.054***
Bare soil (% cover)	-0.053***
Shrub (% cover)	-0.029***
CWD abundance	0.008**	...	0.016*
Post-fire mean summer temperature (MST)	...	-0.027***	...
Topographic wetness index (TWI)	0.007**	0.011**	0.017*
Heat load index (HLI)	-0.007**	-0.008*	...
Slope (°)	-0.007**

Notes: Variable estimates are listed if they were significant in the associated model; "..." indicates variable was not included in the associated model. Asterisks indicate levels of significance: * $P < 0.05$, ** $P < 0.01$, *** $P < 0.001$. Sample size (n) for the count models was 109. For a full list of the predictor variables included in models and their methods of measurement, see Table 2.

values > 0.05 from the Pearson's goodness of fit chi-squared test (Appendix S1: Table S5). Count models also accurately predicted the observations (Spearman's Rank correlation, $\rho = 0.701 - 0.745$).

As indicated by the realizations of the GLM models parameterized to focus on distance from seed source, seedling abundance declined sharply with increasing distance to live seed sources (Fig. 4, Table 5). Shade-intolerant species reached low abundance (< 200 seedlings/ha) past 100 m from live seed source and maintained a low abundance (> 50 seedlings/ha) up to 500 m. Alternatively, shade-tolerant species reached very low abundance (< 50 seedlings/ha) past 100 m from live seed source and became virtually absent past 200 m (Fig. 4). Conservatively, and to associate the above plot-scale findings to patch-scale dispersal, we chose two distance to seed source thresholds (identified from Fig. 4) of 100 and 250 m to respectively represent the distances beyond which severely burned patches may transition into a low-density or non-forest state (e.g., < 250 and < 100 seedlings/ha).

Future forest trajectories: scaling plot to patch scale

We place the preceding data collected at the plot scale, especially the importance of distance to seed source, in the context of landscape-scale fire patterns by identifying the distances of severely burned areas in the broader landscape to patches with live seed source (patches

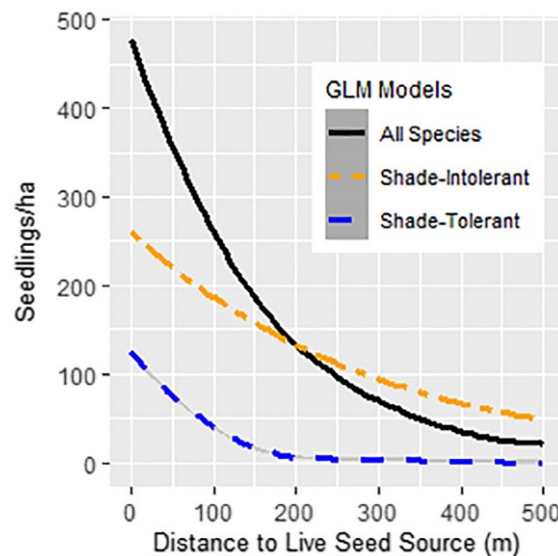


Fig. 4. Post-fire seedling abundance probability as a function of increasing distance to seed source. Final reduced GLMs (Table 5) were used to separately model post-fire abundances of shade-tolerant, shade-intolerant, and all species combined. To reduce the influence of model parameters other than distance to seed source in each probability curve, parameters included in each GLM model were kept at their median value for all burned plots when generating curves.

unburned or burned at low or moderate severities). We found large differences in distance from potential seed source patches to high-severity burn patches when comparing the two study

Table 6. Percentages of the greater study areas burned at a high-severity in relation to their distance to assumed live seed source patches.

Distance to live seed source patch	Mt. Adams Area		Mt. Jefferson Area		Expected seedling density	Potential ecosystem trajectory
	Percentage of high-severity area	Area (ha)	Percentage of high-severity area	Area (ha)		
<100 m	40	6400	64%	7040	>250 seedlings/ha	recovered forest
100–250 m	21	3360	21%	2310	100–250 seedlings/ha	low-density forest
>250 m	39	6240	15%	1650	<100 seedlings/ha	non-forest
Total high-severity area	100	16,000	100%	11,000		

Notes: Percentages of high-severity burned patches were calculated using remotely sensed burn severity (RdNBR) raster data from study area wildfires. Expected seedling densities were calculated from the All Species seedling abundance probability model (Fig. 4). Median pre-fire tree density across all sampled plots was 566 trees/ha.

areas, with 39% of the high-severity burned area at Mt. Adams >250 m from presumed live seed source, but only 15% at Mt. Jefferson (Table 6). The Mt. Adams area also exhibited a greater percentage of cumulative burned area having been burned at least once at high-severity (55%), and a greater maximum distance to seed source (up to 1400 m) compared to Mt. Jefferson (29% and 600m, respectively; Appendix S1: Fig. S6, Table S6). If seedlings indeed fail to recover in severely burned areas at distances of >250 m from live seed source, then approximately 6240 ha of severely burned Mt. Adams areas (39% of high-severity patches, 21% of total wildfire areas) and 1650 ha of severely burned Mt. Jefferson areas (15% of high-severity patches, 4% of total wildfire areas) may fail to recover as forest and instead transition into a non-forest state.

DISCUSSION

Expansive, severe, and repeated wildfires substantially weaken the resilience of moist upper-montane and subalpine conifer forests, based on the evidence from our study in the U.S. Pacific Northwest Central Cascades. Drastically reduced tree regeneration appears to follow from the very large distances between severely burned areas and the closest live seed sources after expansive, high-severity fires burn over large swaths of previously dense forest. Changes in forest structure and composition are indicated by the apparent lesser suitability of formerly dominant, shade-tolerant species in the now more exposed hillslopes burned with any recent high-severity fire (single H, or SIF LH or HL), with fire-tolerant conifers (especially *P. contorta*)

disproportionately increasing in fraction of overall stem density. Our findings highlight that under increasing summer dryness, more expansive, high-severity, and/or short-interval wildfires will likely result in long-lasting effects and large-scale transitions that promote patchy, lower density forests.

Rapid reburns alter post-fire forest structure and seedling composition

In our Central Cascades study areas, reburned SIF plots in both severity sequences (low-high, high-low) were structurally different from forest plots exposed to only a single high- or low-severity fire (e.g., Stevens-Rumann and Morgan 2016). Overall forest structure did not differ between LH and HL SIF sequences, however, except with respect to remnant tree canopy cover (lower for HL) and downed CWD (higher for HL). Considering individual forest structure variables, differences between SIF and single fire effects on overall forest structure were best explained by lower fine-fuel abundance, greater proportion of heavily charred standing trees, and further distances to seed source among reburned plots (Table 3). Overall, our post-fire forest structure results from the Cascades reflect the effects of SIFs observed in other mixed-conifer forests, where rapidly repeated fire progressively consumes dead standing and downed woody biomass (Larson et al. 2013, Stevens-Rumann and Morgan 2016, Donato et al. 2016a).

Although total post-fire seedling abundance in our study areas was not different between LH and HL SIFs, species proportions and composition were different (Table 4, Fig. 3). A low-high SIF sequence appeared to support the

establishment of all conifer species, whereas a high-low SIF sequence primarily supported establishment of pines *P. contorta* and *P. ponderosa*, despite their relatively low pre-fire tree abundance. We intuit that an LH SIF may mimic a single stand-replacing fire, whereas an HL SIF causes mass initial tree mortality, post-fire seeding, and seedling establishment, and then mortality of unprotected or poorly adapted seedlings during the second fire, with little-to-no nearby seed source left to reseed the stand. Thus, only species with seedlings that disperse very far, grow and/or develop sexual maturity fast, and/or are tough enough to survive a low-severity fire (i.e., pines) survive the HL sequence (Enright et al. 2015).

Fire and landscape effects on seed availability and seedling abundance

Expansive and very severe (~100% tree mortality) fire patterns were compounded by subsequent SIFs in our Cascades study areas, which killed seed sources provided by live trees initially unburned or burned at a low/moderate severity (i.e., in fire refugia) and increased the size and contiguity of severely burned patches, further limiting seed source availability. Studies in drier environments (i.e., Northern Rockies) have indicated that SIFs can progressively kill fire refugia but reported tree mortality was lower than what we observed in the Cascades (Larson et al. 2013, Stevens-Rumann and Morgan 2016). This is likely because dry conditions in these other environments promote lower tree densities, increased abundance of fire resistance species, and sparser fine-fuel buildup. Alternatively, fuels from the more climatically moist Cascades forests in our study supported the spread of fire across previously burned forests (seven- or eleven-year fire-return interval) and promoted high-severity fires (>90% tree mortality) in forest patches that initially escaped burning or burned at a lower severity.

Note that when considering the impact of fire on seed source availability, the absolute severity of burns categorized as high severity is important. In US-MTBS, Landsat imagery-based burn severity indices, high-severity fire is generally classified as causing $\geq 75\%$ canopy loss or tree basal area mortality (Miller and Thode 2007, Miller et al. 2009) but, ecologically, the

differences between 75% and nearly or fully 100% mortality can create substantial differences in post-fire conifer regeneration. Even at nearly 100% mortality, scattered surviving trees can serve as crucial legacy seed sources, enabling forest regeneration and impeding or delaying a conversion away from forest (e.g., Donato et al. 2009a). At the landscape scale, the ecological legacy of scattered live trees may not be detected by remotely sensed burn severity indices that use moderate spatial resolution products like Landsat. This indicates that finer spatial resolution imagery products may have greater ecological utility in some forest systems when assessing high-severity fire impacts on post-fire conifer regeneration (e.g., Coop et al. 2019, Downing et al. 2019).

In this study, poor seedling establishment following any high-severity fire (H, LH, or HL) suggested that lacking proximal seed source was the primary control on regeneration. Our seedling abundance models indicated that seedling densities reached very low levels (<50 seedlings/ha) beyond ~100 m from seed source for the pre-fire dominant, shade-tolerant conifer species (*Abies*, *Picea*, *Tsuga*; virtually no recruitment at 200 m) but more than 500 m from seed source for shade-intolerant species (*Pseudotsuga*, *Pinus*, *Larix*; especially *P. contorta*). This was likely due to a mixture of species-specific seed dispersal strategies, adaptive capacities to exposed post-fire hillslope conditions, positions of shade-intolerant legacy trees on high ridgelines or small rock outcrop refugia, surviving canopy seedbanks (e.g., Larson and Franklin 2005), and potential presence (although low abundance) of serotinous cones among *P. contorta*. We observed *P. contorta* seedlings in plots for which live seed sources were >500 m distance, a potential indicator of serotiny, but seedling abundance was typically very low (<50 seedlings/ha). Considering the pre-fire composition of the forests we sampled, *P. contorta* was always a non-dominant species and never occurred as a pure, even-aged stand, as would be expected from mass serotinous re-establishment in the past. These lines of evidence suggest that serotinous cone selection has been poorly expressed in our Cascades study areas (Lotan and Perry 1983, Schoennagel et al. 2003), indicating that *P. contorta* may have limited capacity to recolonize severely and expansively burned

areas in high-elevation forests of the Cascades range, when compared to serotinous *P. contorta* populations elsewhere (i.e., Yellowstone NP; Turner et al. 2019).

In addition to fire severity and extent and interspecific differences in seeding, landscape factors such as post-fire environmental growing conditions, climate and microclimate, herbivory, and competition further constrain post-fire seedling recruitment (Franklin and Hemstrom 1981, Agee 1993, Stevens-Rumann and Morgan 2019). For our central Cascades study areas, landscape and climate factors that were strong predictors of seedling abundance were generally well-aligned with species traits: Shade-tolerant species' seedlings were more abundant in cooler, moister, shadier conditions (e.g., greater canopy cover, higher topographic wetness index, smaller heat load, and lower mean summer temperature), whereas shade-intolerant species were also limited (slightly less so) by dry conditions but also by bare soil and shrub coverage. Shrub competition therefore seemed to preferentially exclude shade-intolerant species (Littlefield 2019, Tubbesing et al. 2020). As climate change increases average temperature and alters snowpack accumulation and timing, our results indicate that conifers in our Cascades study area may generally benefit from earlier spring snowmelt (i.e., longer growing season; Little et al. 1994), but shade-tolerant species may suffer from increasingly hot summers that reduce moisture availability (e.g., Harvey et al. 2016, Andrus et al. 2018).

Cascades forest resilience in the face of changing climate and wildfire patterns

Post-fire forest regeneration can take many successional pathways, and pathways can shift or emerge decades after a wildfire (Donato et al. 2012, Tepley et al. 2014, Gill et al. 2017). Several lines of evidence from this study, however, suggest that the regeneration trends recently observed in our study areas may not deviate significantly in the future. Expansive high-severity fire and very severe fire effects (near 100% tree mortality) have largely removed conifer seed sources from the landscape, with observed regeneration adequate for forest recovery reaching only ~250 m into 600–1400 m radius swaths of the wildfire outlines. Many generations of seedlings grown to maturity could gradually

encroach into these severely burned areas, thereby facilitating the re-establishment of shade-tolerant species over centuries as long as these sites do not rapidly reburn again (Franklin and Hemstrom 1981, Agee 1993, Turner and Romme 1994). Increasing summer aridity with progressive climate change points to more frequent wildfire, however (Abatzoglou and Williams 2016, Abatzoglou et al. 2017), and potentially larger, more severe fires (Cansler and McKenzie 2014) such as those studied here. Future SIFs may continue to perpetuate transitions into low forest densities or even away from forests (Tepley et al. 2018).

While widespread forest composition change and/or forest cover loss may be alarming, our results indicate that altered fire patterns in the Central Cascade Range may be selecting for forest landscapes better adapted to projected future fire regimes and climate conditions. Where prior mid-to-high-elevation Cascades forests experienced 50–200 + yr fire-return intervals and lacked resilience against frequent fire, emerging forests may promote mixed-severity fire patterns and persistence of seed sources via increased dominance by fire-adapted species, lower fuel loads and fuel connectivity, greater abundance of non-forest patches, and lower tree densities (van Wagendonk et al. 2012, Larson et al. 2013, Coop et al. 2016, Stevens-Rumann and Morgan 2016). Ultimately, the altered structure and composition of emerging forest and non-forest patches may confer greater resilience in the face of shifting climate, by synchronizing with new fire regimes and climate conditions (Turner et al. 1993, Johnstone et al. 2016, McWethy et al. 2019). At the landscape scale, these changes may also increase the structural heterogeneity of historically cool and wet mid-to-high-elevation forests (e.g., Cansler et al. 2018).

CONCLUSIONS

Evidence from this study suggests that the resilience of existing mid-to-high-elevation conifer forests in the Cascade Range is negatively impacted by large, severe, and frequent wildfires. Lack of live seed sources within extensively burned fire areas, low post-fire seedling densities, and anticipated shortening of fire-return intervals foretell that burned forests may

transition into a patchy forest or non-forest state, particularly under drier future conditions. The emerging, early seral forests may incorporate a larger proportion of fire-adapted and drought-tolerant conifer species, lower tree densities, lower fuel loads, and more non-forest patches. In contrast to the structure and composition of existing high-density, moist, shade-tolerant species-dominated forests, the attributes of emerging forests may better synchronize with anticipated increases in fire frequency and temperature from climate change. For forest land managers and stakeholders, these adaptive trade-offs must be weighed against the benefits of seeking to maintain (e.g., by replanting) existing forest compositions, which may be poorly adapted to future climate and fire regimes in the long term.

ACKNOWLEDGMENTS

We thank C. Johnson, A. Lefort, B. Michie, and E. Sykes for their assistance collecting field data and performing data entry. Access to conduct fieldwork within our study areas was graciously provided by the Gifford Pinchot National Forest (USFS) and the Confederated Tribes of the Yakima and Warm Springs Nations. We appreciate feedback from Daniel Donato for developing sampling protocols and helpful comments from two anonymous reviewers. Funding for this research was provided from the National Science Foundation (NSF EAR-1738104). A. Holz was additionally supported by NSF Award #1832483.

LITERATURE CITED

Abatzoglou, J. T. 2013. Development of gridded surface meteorological data for ecological applications and modelling. *International Journal of Climatology* 33:121–131.

Abatzoglou, J. T., C. A. Kolden, A. P. Williams, J. A. Lutz, and A. M. S. Smith. 2017. Climatic influences on interannual variability in regional burn severity across western US forests. *International Journal of Wildland Fire* 26:269–275.

Abatzoglou, J. T., and A. P. Williams. 2016. Impact of anthropogenic climate change on wildfire across western US forests. *Proceedings of the National Academy of Sciences of the United States of America* 113:11770–11775.

Abrahamson, I. 2018. Fire Effects Information System (FEIS). U.S. Department of Agriculture, Forest Service, Rocky Mountain Research Station. <https://www.feis-crs.org/feis/>

Agee, J. 1993. Fire ecology of Pacific northwest forests. Island Press, Washington, D.C., USA.

Aickin, M., and H. Gensler. 1996. Adjusting for multiple testing when reporting research results: the Bonferroni vs Holm methods. *American Journal of Public Health* 86:726–728.

Anderson, M. J. 2017. Permutational multivariate analysis of variance (PERMANOVA). Pages 1–15 in N. Balakrishnan, T. Colton, B. Everitt, W. Piegorsch, F. Ruggeri, J. L. Teugels, and I. W. StatsRef, editors. Statistics reference online. John Wiley & Sons, Chichester, UK.

Andrus, R. A., B. J. Harvey, K. C. Rodman, S. J. Hart, and T. T. Veblen. 2018. Moisture availability limits subalpine tree establishment. *Ecology* 99:567–575.

Atzet, T., and L. A. McCrimmon. 1990. Preliminary plant associations of the southern Oregon Cascade Mountain province. U.S. Department of Agriculture, Forest Service, Siskiyou National Forest, Grants Pass, Oregon, USA.

Beven, K. J., and M. J. Kirkby. 1979. A physically based, variable contributing area model of basin hydrology. *Hydrological Sciences Bulletin* 24:43–69.

Boyd, R. 1999. Indians, fire, and the land in the pacific northwest. Oregon State University Press, Corvallis, Oregon, USA.

Brown, J. K. 1974. Handbook for inventorying downed woody material. Pages 1–32. General Technical Report (INT-16). Intermountain Forest and Range Experiment Station, Ogden, Utah, USA.

Buma, B., C. D. Brown, D. C. Donato, J. B. Fontaine, and J. F. Johnstone. 2013. The impacts of changing disturbance regimes on serotinous plant populations and communities. *BioScience* 63:866–876.

Cansler, C. A., and D. McKenzie. 2014. Climate, fire size, and biophysical setting control fire severity and spatial pattern in the northern Cascade Range, USA. *Ecological Applications* 24:1037–1056.

Cansler, C. A., D. McKenzie, and C. B. Halpern. 2018. Fire enhances the complexity of forest structure in alpine treeline ecotones. *Ecosphere* 9:1–21.

Collins, B. M., R. G. Everett, and S. L. Stephens. 2011. Impacts of fire exclusion and recent managed fire on forest structure in old growth Sierra Nevada mixed-conifer forests. *Ecosphere* 2:1–14.

Cook, R. D. 1979. Detection of Influential Observation in Linear Regression. *Technometrics* 19:15–18.

Coop, J. D., T. J. DeLory, W. M. Downing, S. L. Haire, M. A. Krawchuk, C. Miller, M. Parisien, and R. B. Walker. 2019. Contributions of fire refugia to resilient ponderosa pine and dry mixed-conifer forest landscapes. *Ecosphere* 10:1–24.

Coop, J. D., S. A. Parks, S. R. McClernan, and L. M. Holsinger. 2016. Influences of prior wildfires on vegetation response to subsequent fire in a

reburned southwestern landscape. *Ecological Applications* 26:346–354.

Coppoletta, M., K. E. Merriam, and B. M. Collins. 2016. Post-fire vegetation and fuel development influences fire severity patterns in reburns. *Ecological Applications* 26:686–699.

Davis, K. T., S. Z. Dobrowski, P. E. Higuera, Z. A. Holden, T. T. Veblen, M. T. Rother, S. A. Parks, A. Sala, and M. P. Maneta. 2019. Wildfires and climate change push low-elevation forests across a critical climate threshold for tree regeneration. *Proceedings of the National Academy of Sciences of the United States of America* 113:6193–6198.

Dennison, P. E., S. C. Brewer, J. D. Arnold, and M. A. Moritz. 2014. Large wildfire trends in the western United States, 1984–2011. *Geophysical Research Letters* 41:2928–2933.

Donato, D. C., J. L. Campbell, and J. F. Franklin. 2012. Multiple successional pathways and precocity in forest development: Can some forests be born complex? *Journal of Vegetation Science* 23:576–584.

Donato, D. C., J. B. Fontaine, and J. L. Campbell. 2016a. Burning the legacy? Influence of wildfire reburn on dead wood dynamics in a temperate conifer forest. *Ecosphere* 7:1–13.

Donato, D. C., B. J. Harvey, and M. G. Turner. 2016b. Regeneration of montane forests 24 years after the 1988 Yellowstone fires: A fire-catalyzed shift in lower treelines? *Ecosphere* 7:1–16.

Donato, D. C., J. B. Fontaine, J. L. Campbell, W. D. Robinson, J. B. Kauffman, and B. E. Law. 2009a. Conifer regeneration in stand-replacement portions of a large mixed-severity wildfire in the Klamath-Siskiyou Mountains. *Canadian Journal of Forest Research* 39:823–838.

Donato, D. C., J. B. Fontaine, W. D. Robinson, J. B. Kauffman, and B. E. Law. 2009b. Vegetation response to a short interval between high-severity wildfires in a mixed-evergreen forest. *Journal of Ecology* 97:142–154.

Downing, W. M., M. A. Krawchuk, G. W. Meigs, S. L. Haire, J. D. Coop, R. B. Walker, E. Whitman, G. Chong, and C. Miller. 2019. Influence of fire refugia spatial pattern on post-fire forest recovery in Oregon's Blue Mountains. *Landscape Ecology* 34:771–792.

Eidenshink, J., B. Schwind, K. Brewer, Z.-L. Zhu, B. Quayle, and S. Howard. 2007. A project for monitoring trends in burn severity. *Fire Ecology* 3:3–21.

Enright, N. J., J. B. Fontaine, D. M. Bowman, R. A. Bradstock, and R. J. Williams. 2015. Interval squeeze: Altered fire regimes and demographic responses interact to threaten woody species persistence as climate changes. *Frontiers in Ecology and the Environment* 13:265–272.

Franklin, J. F., and C. T. Dyrness. 1973. Natural Vegetation of Oregon and Washington. U.S. Dept. of Agriculture, Forest Service, Pacific Northwest Research Station, Portland, Oregon, USA.

Franklin, J. F., and M. A. Hemstrom. 1981. Aspects of Succession in the Coniferous Forests of the Pacific Northwest. Pages 212–229 in D. C. West, H. H. Shugart, and D. B. Botkin, editors. *Forest Succession: concepts and Application*. Springer, New York, New York, USA.

Gergel, D. R., B. Nijssen, J. T. Abatzoglou, D. P. Lettenmaier, and M. R. Stumbaugh. 2017. Effects of climate change on snowpack and fire potential in the western USA. *Climatic Change* 141:287–299.

Gill, N. S., D. Jarvis, T. T. Veblen, S. T. A. Pickett, and D. Kulakowski. 2017. Is initial post-disturbance regeneration indicative of longer-term trajectories? *Ecosphere* 8:1–13.

Halofsky, J. E., D. L. Peterson, and B. J. Harvey. 2020. Changing wildfire, changing forests: the effects of climate change on fire regimes and vegetation in the Pacific Northwest, USA. *Fire Ecology* 16:1–26.

Hankin, L. E., P. E. Higuera, K. T. Davis, and S. Z. Dobrowski. 2018. Accuracy of node and bud-scar counts for aging two dominant conifers in western North America. *Forest Ecology and Management* 427:365–371.

Harvey, B. J., D. C. Donato, and M. G. Turner. 2014. Recent mountain pine beetle outbreaks, wildfire severity, and postfire tree regeneration in the US Northern Rockies. *Proceedings of the National Academy of Sciences of the United States of America* 111:15120–15125.

Harvey, B. J., D. C. Donato, and M. G. Turner. 2016. High and dry: Post-fire tree seedling establishment in subalpine forests decreases with post-fire drought and large stand-replacing burn patches. *Global Ecology and Biogeography* 25:655–669.

Haugo, R. D., B. S. Kellogg, C. A. Cansler, C. A. Kolden, K. B. Kemp, J. C. Robertson, K. L. Metlen, N. M. Vaillant, and C. M. Restaino. 2019. The missing fire: quantifying human exclusion of wildfire in Pacific Northwest forests. *Ecosphere* 10:1–16.

Hessburg, P. F., et al. 2019. Climate, environment, and disturbance history govern resilience of western North American forests. *Frontiers in Ecology and Evolution* 7:239.

Hildreth, W. 2007. Quaternary magmatism in the Cascades; geologic perspectives. U.S. Geological Survey Professional Paper 1744:125.

Hummel, S., and J. K. Agee. 2003. Western spruce budworm defoliation effects on forest structure and potential fire behavior. *Northwest Science* 77:11.

Johnstone, J. F., et al. 2016. Changing disturbance regimes, ecological memory, and forest resilience.

Frontiers in Ecology and the Environment 14:369–378.

Kemp, K. B., P. E. Higuera, and P. Morgan. 2016. Fire legacies impact conifer regeneration across environmental gradients in the U.S. northern Rockies. *Landscape Ecology* 31:619–636.

Kemp, K. B., P. E. Higuera, P. Morgan, and J. T. Abatzoglou. 2019. Climate will increasingly determine post-fire tree regeneration success in low-elevation forests, Northern Rockies, USA. *Ecosphere* 10:1–17.

Key, C. H., and N. C. Benson. 2006. Landscape assessment: Ground Measure of Severity, the Composite Burn Index; and remote sensing of severity, the normalized burn ratio. In D. C. Lutes, R. E. Keane, J. F. Caratti, C. H. Key, N. C. Benson, S. Sutherland, and L. J. Gangi, editors. FIREMON: fire effects monitoring and inventory system. USDA Forest Service, Rocky Mountain Research Station, Ogden, Utah, USA.

Krawchuk, M. A., and M. A. Moritz. 2011. Constraints on global fire activity vary across a resource gradient. *Ecology* 92:121–132.

LANDFIRE. 2010. Fire Regime Groups. LANDFIRE 1.2.0. U.S. Department of the Interior, Geological Survey. <https://landfire.cr.usgs.gov/frg.php>

Larson, A. J., R. T. Belote, C. A. Cansler, S. A. Parks, and M. S. Dietz. 2013. Latent resilience in ponderosa pine forest: effects of resumed frequent fire. *Ecological Applications* 23:1243–1249.

Larson, A. J., and J. F. Franklin. 2005. Patterns of conifer tree regeneration following an autumn wildfire event in the western Oregon Cascade Range, USA. *Forest Ecology and Management* 218:25–36.

Little, R. L., D. L. Peterson, and L. L. Conquest. 1994. Regeneration of subalpine fir (*Abies lasiocarpa*) following fire: effects of climate and other factors. *Canadian Journal of Forest Research* 24:934–944.

Littlefield, C. E. 2019. Topography and post-fire climatic conditions shape spatio-temporal patterns of conifer establishment and growth. *Fire Ecology* 15:34.

Lotan, J. E., and D. A. Perry. 1983. Ecology and regeneration of lodgepole pine. Agricultural Handbook 606. U.S. Department of Agriculture, Forest Service, Washington, D.C., USA.

McCune, B., and D. Keon. 2002. Equations for potential annual direct incident radiation and heat load. *Journal of Vegetation Science* 13:603–606.

McKenzie, D., and J. S. Littell. 2017. Climate change and the eco-hydrology of fire: Will area burned increase in a warming western USA? *Ecological Applications* 27:26–36.

McWethy, D. B., et al. 2019. Rethinking resilience to wildfire. *Nature Sustainability* 2:797–804.

Meigs, G. W., R. E. Kennedy, A. N. Gray, and M. J. Gregory. 2015a. Spatiotemporal dynamics of recent mountain pine beetle and western spruce budworm outbreaks across the Pacific Northwest Region, USA. *Forest Ecology and Management* 339:71–86.

Meigs, G. W., J. L. Campbell, H. S. Zald, J. D. Bailey, D. C. Shaw, and R. E. Kennedy. 2015b. Does wildfire likelihood increase following insect outbreaks in conifer forests? *Ecosphere* 6:1–24.

Merschel, A. G., T. A. Spies, and E. K. Heyerdahl. 2014. Mixed-conifer forests of central Oregon: Effects of logging and fire exclusion vary with environment. *Ecological Applications* 24:1670–1688.

Miller, J. D., E. E. Knapp, C. H. Key, C. N. Skinner, C. J. Isbell, R. M. Creasy, and J. W. Sherlock. 2009. Calibration and validation of the relative differenced Normalized Burn Ratio (RdNBR) to three measures of fire severity in the Sierra Nevada and Klamath Mountains, California, USA. *Remote Sensing of Environment* 113:645–656.

Miller, J. D., and A. E. Thode. 2007. Quantifying burn severity in a heterogeneous landscape with a relative version of the delta Normalized Burn Ratio (dNBR). *Remote Sensing of Environment* 109:66–80.

Naficy, C., A. Sala, E. G. Keeling, J. Graham, and T. H. DeLuca. 2010. Interactive effects of historical logging and fire exclusion on ponderosa pine forest structure in the northern Rockies. *Ecological Applications* 20:1851–1864.

Oksanen, J., et al. 2018. vegan: Community Ecology Package. R package version 2.5-3. <https://CRAN.R-project.org/package=vegan>

Peters, G. 2018. userfriendlyscience: quantitative Analysis Made Accessible. <https://doi.org/10.17605/osf.io/txequ>

PRISM. 2018. 30-Year Normals. Oregon State University, Corvallis, Oregon, USA.

R Development Core Team. 2017. R: a language and environment for statistical computing. R Foundation for Statistical Computing, Vienna, Austria.

Raffa, K. F., B. H. Aukema, B. J. Bentz, A. L. Carroll, J. A. Hicke, M. G. Turner, and W. H. Romme. 2008. Cross-scale drivers of natural disturbances prone to anthropogenic amplification: the dynamics of bark beetle eruptions. *BioScience* 58:501–517.

Reilly, M. J., C. J. Dunn, G. W. Meigs, T. A. Spies, R. E. Kennedy, J. D. Bailey, and K. Briggs. 2017. Contemporary patterns of fire extent and severity in forests of the Pacific Northwest, USA (1985–2010). *Ecosphere* 8:1–28.

Schoennagel, T., M. G. Turner, and W. H. Romme. 2003. The influence of fire interval and serotiny on post-fire lodgepole pine density in Yellowstone National Park. *Ecology* 84:2967–2978.

SnoDAS. 2004. Snow Data Assimilation System (SnoDAS) Data Products at NSIDC, Version 1. Snow

Water Equivalent. NSIDC: National Snow and Ice Data Center, Boulder, Colorado USA.

Steen-Adams, M. M., S. Charnley, R. J. McLain, M. D. O. Adams, and K. L. Wendel. 2019. Traditional knowledge of fire use by the Confederated Tribes of Warm Springs in the eastside Cascades of Oregon. *Forest Ecology and Management* 450:117405.

Stevens-Rumann, C. S., K. B. Kemp, P. E. Higuera, B. J. Harvey, M. T. Rother, D. C. Donato, P. Morgan, and T. T. Veblen. 2018. Evidence for declining forest resilience to wildfires under climate change. *Ecology Letters* 21:243–252.

Stevens-Rumann, C., and P. Morgan. 2016. Repeated wildfires alter forest recovery of mixed-conifer ecosystems. *Ecological Applications* 26:1842–1853.

Stevens-Rumann, C. S., and P. Morgan. 2019. Tree regeneration following wildfires in the western US: a review. *Fire Ecology* 15:15.

Stine, P., et al. 2014. The ecology and management of moist mixed-conifer forests in eastern Oregon and Washington: a synthesis of the relevant biophysical science and implications for future land management. U.S. Department of Agriculture, Forest Service, Pacific Northwest Research Station, Portland, Oregon, USA.

Tepley, A. J., F. J. Swanson, and T. A. Spies. 2013. Fire-mediated pathways of stand development in Douglas-fir/western hemlock forests of the Pacific Northwest, USA. *Ecology* 94:1729–1743.

Tepley, A. J., F. J. Swanson, and T. A. Spies. 2014. Post-fire tree establishment and early cohort development in conifer forests of the western Cascades of Oregon, USA. *Ecosphere* 5:23.

Tepley, A. J., E. Thomann, T. T. Veblen, G. L. W. Perry, A. Holz, J. Paritsis, T. Kitzberger, and K. J. Anderson-Teixeira. 2018. Influences of fire-vegetation feedbacks and post-fire recovery rates on forest landscape vulnerability to altered fire regimes. *Journal of Ecology* 106:1925–1940.

Tubbesing, C. L., R. A. York, S. L. Stephens, and J. J. Battles. 2020. Rethinking fire-adapted species in an altered fire regime. *Ecosphere* 11:1–15.

Turner, M. G., K. H. Braziunas, W. D. Hansen, and B. J. Harvey. 2019. Short-interval severe fire erodes the resilience of subalpine lodgepole pine forests. *Proceedings of the National Academy of Sciences of the United States of America* 116:11319–11328.

Turner, M. G., and W. H. Romme. 1994. Landscape dynamics in crown fire ecosystems. *Landscape Ecology* 9:59–77.

Turner, M. G., W. H. Romme, R. H. Gardner, R. V. O'Neill, and T. K. Kratz. 1993. A revised concept of landscape equilibrium: disturbance and stability on scaled landscapes. *Landscape Ecology* 8:213–227.

Urza, A. K., and J. S. Sibold. 2013. Nondestructive aging of post-fire seedlings for four Conifer species in Northwestern Montana. *Western Journal of Applied Forestry* 28:22–29.

USDA. 2018. Web Soil Survey. US Department of Agriculture. <https://websoilsurvey.sc.egov.usda.gov/>

van Wagendonk, J. W., K. A. van Wagendonk, and A. E. Thode. 2012. Factors Associated with the severity of intersecting fires in Yosemite National Park, California, USA. *Fire Ecology* 7:11–31.

Venables, W. N., and B. D. Ripley. 2002. Modern applied statistics. Fourth edition. Springer, New York, New York, USA.

Wang, T., A. Hamann, D. Spittlehouse, and C. Carroll. 2016. Locally downscaled and spatially customizable climate data for historical and future periods for North America. *PLoS One* 11:1–17.

Westerling, A. L. 2016. Increasing western US forest wildfire activity: sensitivity to changes in the timing of spring. *Philosophical Transactions of the Royal Society B: Biological Sciences* 371:20150178.

Whittier, T. R., and A. N. Gray. 2016. Tree mortality based fire severity classification for forest inventories: a Pacific Northwest national forests example. *Forest Ecology and Management* 359:199–209.

Wickham, H. 2016. *ggplot2: elegant graphics for data analysis*. Springer-Verlag, New York, New York, USA. <https://ggplot2.tidyverse.org>

Zuur, A. F., E. N. Ieno, and C. S. Elphick. 2010. A protocol for data exploration to avoid common statistical problems: data exploration. *Methods in Ecology and Evolution* 1:3–14.

Zuur, A. F., A. A. Savaliev, and E. N. Ieno. 2012. *Zero inflated models and generalized linear mixed models with R*. Highland Statistics, Newburg, UK.

SUPPORTING INFORMATION

Additional Supporting Information may be found online at: <http://onlinelibrary.wiley.com/doi/10.1002/ecs2.3247/full>